RSC Advances



PAPER View Article Online View Journal | View Issue



Cite this: RSC Adv., 2025, 15, 40188

Investigating the enhancement of the rate of CO₂ capture of CaO in the presence of steam through ¹⁸O isotope labeling: pitfalls and findings

Felix Donat * and Christoph R. Müller * *

The reaction of CO_2 with CaO to form $CaCO_3$ can be used to remove CO_2 from gas streams in post-combustion CO_2 capture schemes at high temperatures (>600 °C). The rate of CO_2 uptake is increased substantially in the presence of steam, but the underlying reasons have not yet been resolved, although several explanations have been proposed in the literature. In our study we generated steam from labeled water ($H_2^{18}O$) to track ^{18}O in the gas and solid products using mass spectrometry and Raman spectroscopy, aiming to understand whether oxygen (or OH^-) contained in H_2O participates directly in the formation of $CaCO_3$. Unfortunately, it was not possible to investigate the interaction of $H_2^{18}O$ with $CaO/CaCO_3$ isolated, because in the presence of CO_2 oxygen was exchanged between H_2O and CO_2 in the high-temperature reaction chamber of the thermogravimetric analyzer before any interaction of the gaseous reactants with the sorbent. ^{18}O was detected in the $CaCO_3$ product, but it originated from ^{18}O in CO_2 rather than H_2O . Yet, our measurements suggest that oxygen exchange occurs between $CaCO_3$ and CO_3 under reaction conditions, but not between $CaCO_3$ and CO_3 , which may motivate further investigations.

Received 13th July 2025 Accepted 14th October 2025

DOI: 10.1039/d5ra05023e

rsc.li/rsc-advances

1. Introduction

Calcium looping is a promising technique to capture CO₂ from point sources at high efficiency. 1-3 On a process level, CaO-based sorbents react with CO2 contained in flue gases from combustion or other CO₂ emitting processes at temperatures between 600 and 700 °C (carbonation), removing up to 90% of the CO₂. 4-6 The resulting CaCO₃ is decomposed subsequently at a high temperature (>900 °C) to release CO2 and recover the CaO-based sorbent (calcination). The CO2 obtained from the decomposition of CaCO₃ can be compressed and stored underground, or used as a feedstock in chemical conversion processes.^{7,8} CaObased sorbents tend to lose their activity for fast CO₂ sorption with increasing number of cycles of CO2 sorption and release. The high theoretical CO₂ uptake capacity of 0.78 g CO₂ per g CaO is practically not achievable owing to sintering that reduces surface area and pore volume.3 During carbonation, CO2 molecules need to diffuse through a network of narrow pores within the sorbent particle, and as pores close due to the builtup of the product CaCO₃, the rate of CO₂ sorption decreases; some of the CaO contained in the sorbent particle is not even accessible for CO₂ at all within typical residence times.

Interestingly, small quantities of steam (even <1 vol%) present in the CO_2 -containing gas increase the rate of CO_2

Laboratory of Energy Science and Engineering, Department of Mechanical and Process Engineering, ETH Zürich, Leonhardstrasse 21, 8092 Zürich, Switzerland. E-mail: donatf@ethz.ch; muelchri@ethz.ch sorption of CaO (*viz.*, the rate of CaCO₃ formation). The increase is most significant when intraparticle diffusion controls the rate of CO₂ sorption, indicating that steam influences the diffusional transport of CO₂ within the sorbent. Steam is also known to accelerate the decomposition of CaCO₃ (ref. 10–13) and affect the structural and morphological properties of the CaO formed, ^{11,14,15} resulting sometimes even in an increase in mechanical strength. ^{16,17} It has been observed that the CO₂ uptake of limestone-derived CaO was improved under dry conditions when the decomposition of CaCO₃ in the previous reaction step was performed in the presence of steam, because the resulting pore structure of CaO was more favorable for fast CO₂ sorption, offering less intraparticle diffusional resistance for CO₂ molecules. ^{9,18}

Despite numerous studies, the mechanism of the enhancing effect of steam during CO₂ sorption at high temperatures (>600 °C) is still not fully understood. An overview of relevant investigations concerning the effect of steam on the carbonation reaction has been provided recently by Dunstan *et al.*,³ building up on earlier work by Zhang *et al.*¹⁹ Several studies have hypothesized that OH⁻ groups originating from the dissociative adsorption of steam on the surface of CaO play an important role,^{20,21} but no experimental evidence has been provided yet; note that the phase Ca(OH)₂ is thermodynamically not stable at ambient pressure at temperatures >550 °C, and is therefore not expected to contribute as an intermediate species to the faster CO₂ sorption. Coverage of the CaO surface with OH⁻ would not explain why the enhancement of the rate of CO₂ sorption is

Paper

most noticeable once a significant amount of CaO has been converted into CaCO3 already. Li et al. 22,23 proposed a mechanism that considers diffusional transport in the CaCO₃ product layer: H₂O molecules dissociate on the CaCO₃ surface (gas-solid interface), forming H⁺ and OH⁻. Given the small radius of H⁺, it diffuses rapidly through the CaCO₃ product to the CaO-CaCO₃ interface, where it reacts with O²⁻ to form OH⁻. OH⁻ diffuses outwards to the CaCO₃-gas interface to react with CO₂, forming CO₃²⁻ that diffuses inwards through the CaCO₃ product layer to the CaO-CaCO3 interface, where new CaCO3 is ultimately formed. OH⁻ diffusion is faster than O²⁻ diffusion under dry conditions and so is assumed to explain the increase in the rate of CaCO₃ formation in the presence of steam; note that the counter-current diffusion mechanism of CO32- and O2- under dry conditions was experimentally demonstrated by Sun et al.24 through an inert marker experiment. Strictly speaking, it is not the OH⁻ on the surface (which originates from the dissociation of H₂O) that participates in the formation of CaCO₃, but the OH⁻ formed following proton (H⁺) diffusion and reaction with O². This is different from recent density functional theory (DFT) results to understand the promotion of CO2 sorption on Li₄SiO₄-based sorbents with water vapor, which conclude that surface OH⁻ contributes to the enhanced CO₂ uptake.²⁵

An interesting body of literature deals with the diffusion of oxygen, hydrogen and carbon in minerals (including the calcite polymorph of CaCO₃), relevant to many geological processes such as fluid-rock interactions or the growth of minerals.26 Using isotope tracers such as ¹⁸O or ¹³C and ion microprobes, it was found that volume/lattice diffusion of oxygen is improved substantially (by at least 1-2 orders of magnitude) in the presence of water, whereas carbon and cations diffusion are hardly affected by the presence of water (400-800 °C, total pressure 0.1-350 MPa).27,28 In many types of minerals such as quartz, feldspars and calcite, molecular H2O rather than OH was identified as the dominant diffusing species bearing oxygen under hydrothermal conditions, as oxygen transport depended linearly on water fugacity.29-31 The rate of diffusion of oxygen is believed to be controlled by reactions at the surface of calcite, 32,33 which may be relevant also for typical calcium looping conditions. Specifically, adsorption of H₂O and the creation of vacancy defects at the surface explain the dependence of the diffusivity of oxygen on the fugacity of water. The dissociation of water on the calcite surface supplies protons that hydrolyze and weaken C-O bonds in calcite akin to Si-O bonds in silicates, and thus makes oxygen exchange between H₂O and structurally bound oxygens energetically favorable.^{30,32} Carbonate ion (CO₃²⁻) was identified as the dominant carboncontaining diffusing species in calcite from measurements of the oxygen/carbon exchange rate ratio.34 Furthermore, there has been little evidence that hydrogen itself diffuses into calcite, and it has been concluded that hydrogen cannot be responsible for the increased diffusivity of oxygen in calcite.32

In this work, we investigate whether oxygen contained in steam (or OH⁻ groups originating from steam) is involved directly in the formation of the CaCO₃ product. Such involvement (or non-involvement) would shed light on the sequence of reactions that lead to CaCO₃ formation, and help understand

whether steam contributes to the increased rate of CO_2 uptake as a carrier of oxygen. Thus, we co-feed steam containing the oxygen isotope ^{18}O (*i.e.*, $H_2^{18}O$) during the carbonation reaction, use Raman spectroscopy to detect ^{18}O in the $CaCO_3$ formed, and mass spectrometry to detect ^{18}O in the CO_2 released from the $CaCO_3$.

If, as proposed by Li et al., 23 OH groups originating from the reaction of H⁺ (from the dissociation of H₂¹⁸O) with O²⁻ at the CaO-CaCO3 interface interact with CO2 molecules and form CO₃²⁻, then any CO₂ released during the decomposition of CaCO₃ should not contain ¹⁸O because the origin of O²⁻ is not the H₂¹⁸O molecule. If, however, oxygen or OH⁻ groups from H₂¹⁸O on the surface of CaO/CaCO₃ (the solid-gas interface) participate in the formation of CO₃²⁻, then the CO₂ released during the decomposition of CaCO₃ should indeed contain ¹⁸O, e.g., as C16O18O or C18O2. Generally, any indication of 18O in the CO2 released from the sorbent (beyond their natural abundance) would imply that steam participates actively in the formation of CaCO3 rather than acting as a catalyst or functioning by other means; this would also disprove the mechanism proposed by Li et al. as the only pathway by which steam enhances the rate of CO2 sorption/CaCO3 formation. Not detecting 18O in the CO2 released from the decomposition of CaCO₃ would not directly prove the mechanism proposed by Li et al. but demonstrate that oxygen or OH groups originating from steam do not contribute to the formation of CO₃²⁻ and

Experimental materials and methods

2.1 CaO-based sorbent

Natural limestone (Rheinkalk, >98 wt% CaCO₃, surface area $\sim 1~\text{m}^2~\text{g}^{-1}$) was used in all experiments as the precursor for CaO. Prior to the experiments using a thermogravimetric analyzer (TGA), limestone particles were calcined at 900 °C in N_2 for 30 min, followed by cooling to room temperature. The sorbent particles were then sieved to 150–212 μm to ensure that in the TGA experiments their packing inside the crucible had no influence on the CO₂ transport that would otherwise affect the observed rate of CO₂ uptake. 35

2.2 Material characterization

Raman spectroscopy on powdery, partially carbonated samples was performed using a Thermo Scientific DXR Raman microscope (laser wavelength 455 nm). The crystalline phases of the powdery samples were analyzed \emph{via} X-ray diffraction (XRD) using a PANalytical Empyrean X-ray diffractometer (Cu K α radiation, 45 kV and 40 mA) equipped with a X'Celerator Scientific ultrafast line detector and Bragg–Brentano HD incident beam optics.

2.3 Thermogravimetric analyzer (TGA) setup

CO₂ sorption experiments were carried out using a TGA (Mettler Toledo, TGA/DSC1, volume of the high-temperature reaction chamber: 16 ml) following the same principal protocol: sorbent

RSC Advances

particles (15-20 mg) were loaded into a shallow, 30 µl crucible made of aluminum oxide and heated to 900 °C in N2. After 15 min, the temperature was reduced to 650 °C (CO₂ sorption temperature). The gas atmosphere was changed from pure N2 to 15 vol% CO₂/N₂ for 20 min for CO₂ sorption in the presence or absence of steam. 15 vol% CO2/N2 was used to reflect typical CO₂ concentrations in post-combustion CO₂ capture, and enable comparison with previous works. Subsequently, the gas atmosphere was changed back to N2, and the temperature was increased to 950 °C (CO2 release temperature). After holding at 950 °C for 10 min, the temperature was decreased to 650 °C for a new reaction cycle to begin. Note that only the CO₂ sorption stage was performed in the presence of steam, but not the heating, cooling and CO2 release stages. Heating and cooling rates were 30 °C min⁻¹ and the total flow rate was always 100 ml min⁻¹ (incl. 25 ml min⁻¹ of dry N₂ purge over the microbalance), as measured and controlled at normal temperature and pressure by mass flow controllers (Bronkhorst, EL-FLOW).

Steam was generated by flowing 60 ml min⁻¹ of N₂ (or 60 ml per min N₂ and 15 ml per min CO₂, see details below) through a small gas washing bottle (volume 5 ml) filled with deionized water or water containing the isotope ¹⁸O (labeled water, H₂ ¹⁸O, 97 atom% ¹⁸O, Sigma-Aldrich) at ambient temperature, as shown in Fig. 1. Separate measurements using a humidity probe (Sensirion, SHT31) showed ~90% saturation of the gas stream with water. The temperature of the laboratory (and the water in the gas washing bottle) varied between 22 and 24 °C, and hence the steam concentration in the reaction chamber of the TGA was \sim 1.5-2.0 vol% (a larger flow rate through the saturator and a higher ambient temperature result in a higher steam concentration). A solenoid valve synchronized with the temperature program of the TGA enabled the sharp separation of dry and humid gas environments. In addition to the two types of water used (deionized water or water containing the isotope ¹⁸O), two options for mixing CO₂ and steam/water prior to entering the TGA reaction chamber were investigated (Fig. 1). The first option aimed at mixing CO2 and steam in the gas phase; thus, pure N2 flowed through the saturator and was mixed with the CO2 stream after the saturator just before entering the reaction chamber of the TGA. For the second option, a mixture of N2 and CO2 flowed through the saturator, such that also CO2 was mixed with liquid water to generate steam; this option was always used when deionized water was used.

The gas outlet from the TGA was connected directly to a mass spectrometer (MS, MKS Cirrus 3) through a heated transfer line

Table 1 Relative intensities of the different mass-to-charge ratios (m/ z) for the relevant gas species36

| Mass-to-charge ratio (m/z) | Species | | | | | |
|------------------------------|---------|-------------------------|--------------------|-------------|-----------------------------------|-------------|
| | | ${\rm H_2}^{18}{\rm O}$ | $^{16}{\rm O}_{2}$ | $C^{16}O_2$ | C ¹⁶ O ¹⁸ O | $C^{18}O_2$ |
| 18 | 100 | n/a | 0 | 0 | n/a | n/a |
| 20 | 0.3 | 100 | 0 | 0 | n/a | n/a |
| 32 | 0 | 0 | 100 | 0 | n/a | n/a |
| 44 | 0 | 0 | 0 | 100 | n/a | n/a |
| 46 | 0 | 0 | 0 | 0.4 | 100 | n/a |
| 48 | 0 | 0 | 0 | 0 | n/a | 100 |

to analyze the composition of the product gases, and to detect ¹⁸O in CO₂ and H₂O (see Table 1). When changing the atmosphere from 15 vol% CO₂/N₂ to pure N₂ after the CO₂ sorption stage, the release of CO2 from the sample did not occur immediately, but required higher temperatures (>700 °C) for kinetic reasons. The MS was sufficiently fast to resolve the two events of (i) a decreasing CO2 signal due to the change in atmosphere from 15 vol% CO2/N2 to pure N2, and (ii) an increasing CO2 signal due to the release of CO2 from the sample during the decomposition reaction when heating to 950 °C.

3. Results

TGA cyclic performance and MS signals 3.1

Fig. 2a and b compare the normalized sample mass of the limestone-based sorbent under dry and humid conditions over five cycles of CO₂ sorption and release. A value of one implies that the sorbent is calcined completely, and any increase in normalized sample mass is due to the sorption of CO2 when the material transitions from CaO to CaCO3. The difference between the normalized sample mass and one is thus equivalent to the CO₂ uptake in g CO₂ per g sorbent, and it can reach a maximum value of \sim 0.77 for this particular sorbent for the case that all CaO is converted into CaCO3 (the normalized sample mass would then show a value of 1.77).

Under dry conditions, the CO2 uptake observed at the end of the CO₂ sorption stage decreased gradually with cycle number, as is commonly observed for limestone-based sorbents.37 Under humid conditions, the CO₂ uptake was significantly higher and even increased slightly with cycle number. Whether deionized water, labeled water, or a mixture of deionized and labeled water was used during carbonation did not affect the observed rate and extent of the CO₂ uptake during the five cycles of CO₂

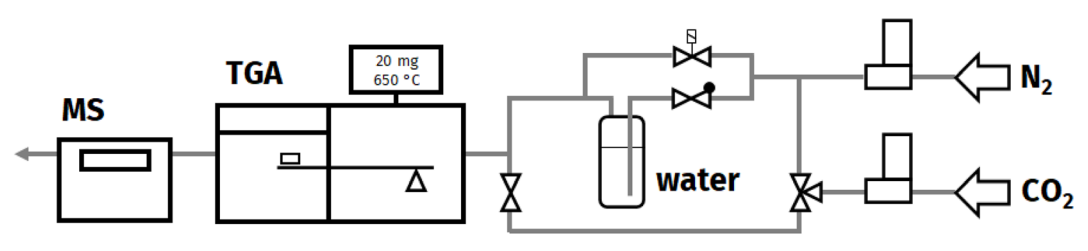


Fig. 1 Schematic illustration of the experimental setup using TGA and MS, and the steam injection system.

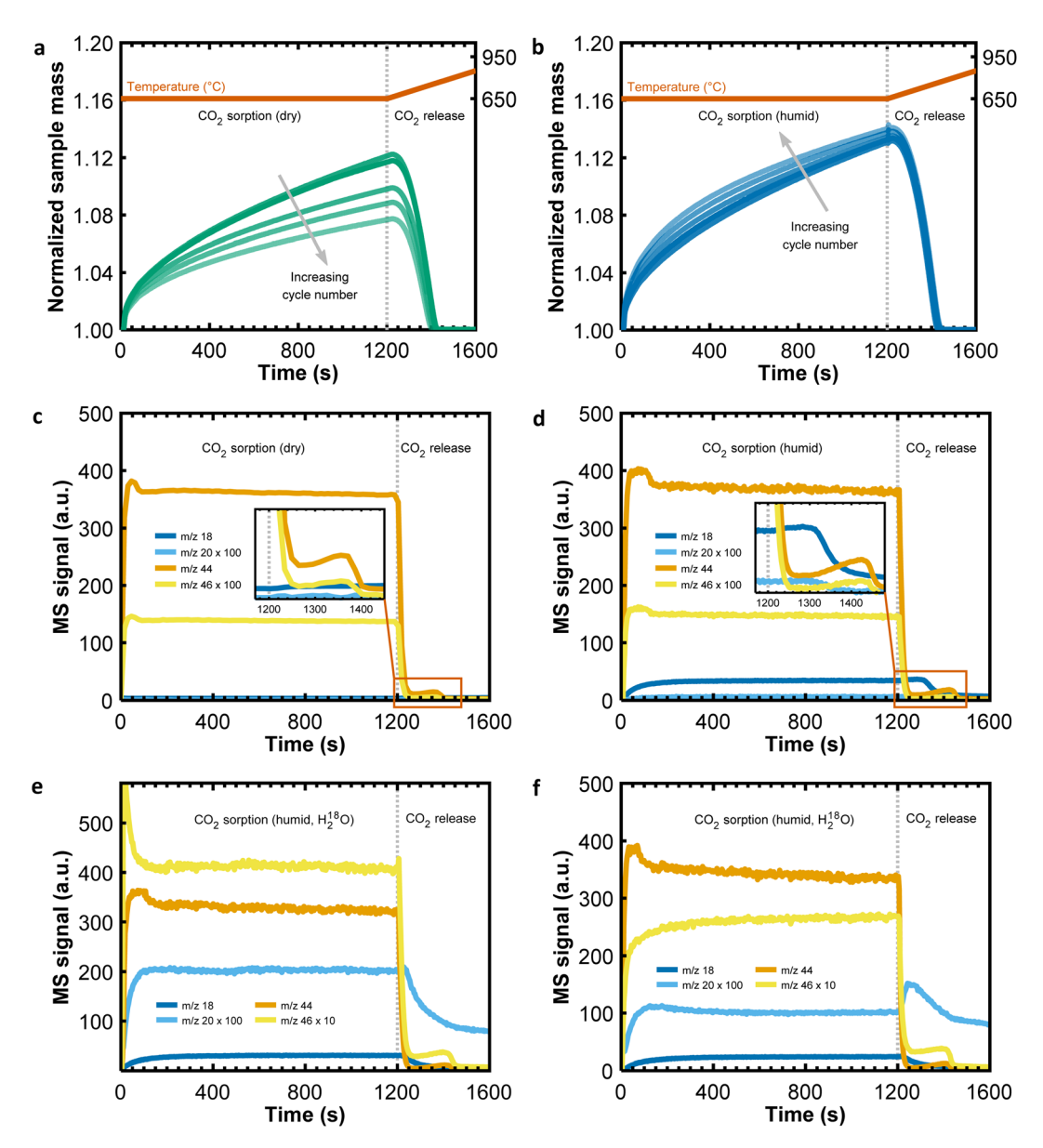


Fig. 2 Results from the TGA experiments over five cycles of CO_2 sorption and release using a limestone-based sorbent. (a) CO_2 sorption in a dry CO_2 -containing atmosphere. (b) CO_2 sorption in a humid CO_2 -containing atmosphere using deionized water. (c) and (d) Show the MS signals corresponding to the TGA measurements shown in (a) and (b) for the fifth carbonation cycle. (e) and (f) Show the MS signals that correspond to the same cycling experiment shown in (b), but using steam derived from labeled water ($H_2^{-18}O$) instead of deionized water; in (e) both N_2 and CO_2 flowed through the saturator, whereas in (f) only N_2 flowed through the saturator.

sorption and release (supplementary plots in Fig. 4a and b). Also, small variations in the steam concentration (due to minor temperature variations in the laboratory, the different flow rates of gas through the saturator, or the water level in the saturator) had no noticeable effect on the observed CO₂ uptake. Adding steam to the CO₂-containing atmosphere during the CO₂ sorption stage increased the rate of CO₂ sorption even after a substantial amount of CaCO₃ had been formed already under dry conditions (shown below in Fig. 4c). From Fig. 2a and b it is apparent that CO₂ was released from the sorbent before the CO₂ release temperature of 950 °C was reached, but whether steam was present during the CO₂ sorption stage or not did not affect the rate of the subsequent decomposition of CaCO₃ noticeably.

Fig. 2c and d plot the MS signals under dry and humid conditions, respectively, recorded during the fifth reaction cycle, whereas Fig. 2e and f show the MS signals recorded during the fifth reaction cycle when labeled water (${\rm H_2}^{18}{\rm O}$) instead of deionized water (${\rm H_2}^{16}{\rm O}$) was used to generate steam; note that the MS signals are plotted on a linear scale and that the intensity of some signals (*e.g.*, m/z 20 or m/z 46) was magnified for illustration purposes. Under dry conditions (Fig. 2c) signals due to ${\rm CO_2}$ (m/z 44 and 46) were observed, whereas in the presence of unlabeled steam (containing only $^{16}{\rm O}$, Fig. 2d) also signals due to ${\rm H_2O}$ (m/z 18 and 20) were observed. When changing the atmosphere from (dry or humid) 15 vol% ${\rm CO_2/N_2}$ to pure ${\rm N_2}$ at the end of the carbonation stage,

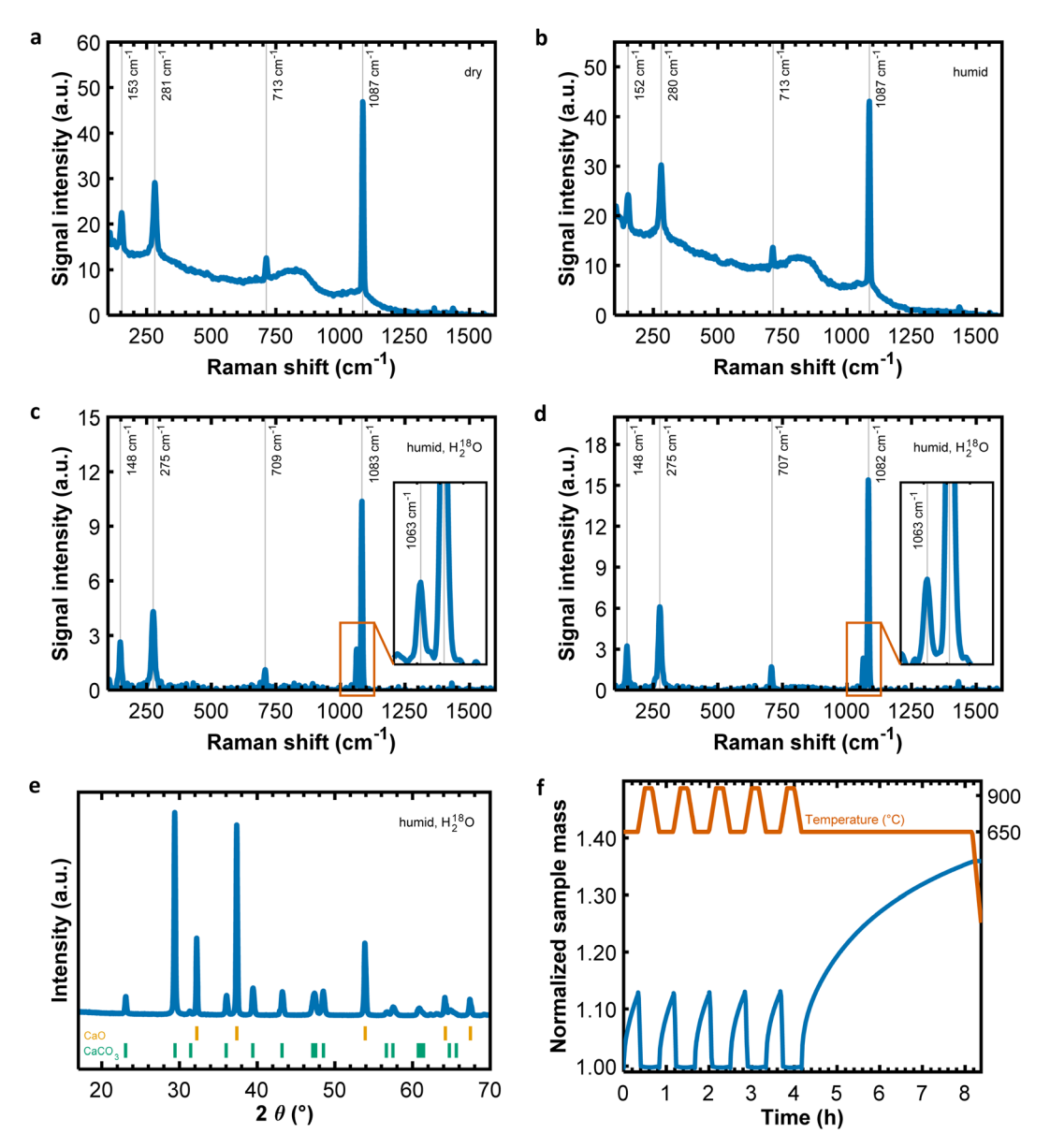


Fig. 3 (a)–(d) Raman spectroscopy measurements of partially carbonated sorbents after five reaction cycles plus an extended carbonation for 4 h. The order of the plots is the same as in Fig. 2c–f, corresponding to the different atmospheres during the carbonation stage (dry, humid ($H_2^{16}O$), humid ($H_2^{18}O$) with N_2 and N_2 flowing through the saturator, and humid ($N_2^{18}O$) with only N_2 flowing through the saturator). (e) XRD measurement of a partially carbonated sorbent (using labeled water $N_2^{18}O$). (f) Example of a TGA experiment (here using deionized water $N_2^{16}O$) to produce the samples for the subsequent analyses shown in (a)–(e).

there was a rapid decrease in the signal due to CO_2 (m/z 44 and 46, seen in all of the Fig. 2c-f), followed by a slight, short increase due to the release of CO_2 from the material when the temperature approached ~700 °C. Under humid conditions (Fig. 2d-f), the CO_2 uptake was greater, and so it took slightly longer to release all CO_2 captured during the subsequent heating step in dry N_2 (this is seen also from the mass changes in Fig. 2a and b). Interestingly, when steam was present during the CO_2 sorption stage at 650 °C, the MS signals due to steam (m/z 18 and 20) did not return to zero immediately after the atmosphere had been changed back to dry N_2 , and even increased slightly with increasing temperature (this is seen best in the inset of Fig. 2d for m/z 18 or in Fig. 2f for m/z 20). Blank

measurements without any sample in the crucible show similar trends (Fig. 5a and b), implying that the slow decrease of the MS signals due to steam (m/z 18 and 20) when changing the atmosphere back to dry N₂ was related to the experimental setup rather than any material-related effects. Importantly, the MS signals in Fig. 2e and f show the release of CO₂ containing ¹⁸O during the CO₂ release stage ($C^{16}O^{18}O$, m/z 46), indicating that a substantial amount of CaCO₃ containing one ¹⁸O had formed during the previous carbonation stage in the presence of H₂ ¹⁸O (note the difference in magnification of m/z 46 compared to Fig. 2d). At first sight, this observation would confirm that steam indeed participates actively in the formation of CaCO₃, as discussed in the introduction.

Paper

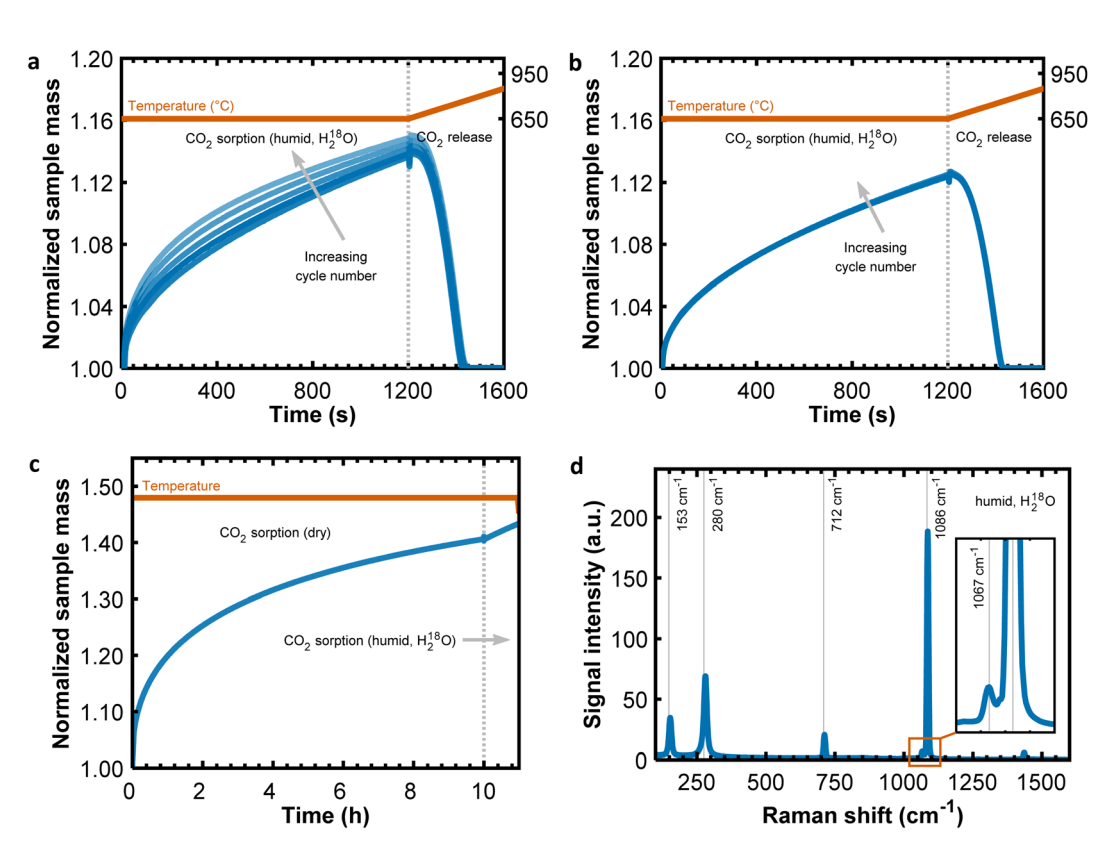


Fig. 4 Results from TGA experiments of CO_2 sorption and release using a limestone-based sorbent. (a) CO_2 sorption in a humid CO_2 -containing atmosphere using steam derived labeled water ($H_2^{18}O$) with both N_2 and CO_2 flowing through the saturator. (b) CO_2 sorption in a humid CO_2 -containing atmosphere using labeled water ($H_2^{18}O$) with only N_2 flowing through the saturator, two cycles only. (c) Long CO_2 sorption under dry conditions at 650 °C; after 10 h CO_2 sorption continued using steam derived from labeled water ($H_2^{18}O$), showing an increase in the rate of CO_2 uptake. (d) Raman spectroscopy measurements of the sample shown in (c).

3.2 Oxygen exchange between steam and carbon dioxide at elevated temperature

However, the release of CO₂ containing 18 O (16 O 18 O, m/z 46) is not sufficient to confirm the participation of steam in the formation of calcium carbonate, because the origin of ¹⁸O is not clear yet. From control experiments (Fig. 6) and literature reports for CaCO₃ (ref. 38) and MgCO₃,³⁹ there is no indication that oxygen of crystalline CaCO₃ would be exchanged with ¹⁸O contained in gas-phase H₂O or CO₂ that would have resulted in the formation CaC18O16O2. However, although almost pure labeled water (>97 atom% 18O) was used in the measurements shown in Fig. 2e and f, the intensity of m/z 18 (due to $H_2^{16}O$) was significantly greater than the intensity of m/z 20 (due to $H_2^{18}O$). Similarly, the intensity of m/z 46 (due to $C^{16}O^{18}O$) relative to m/z44 (due to C¹⁶O₂, for simplicity written as CO₂) during the CO₂ sorption stage was greater than expected from Table 1 or Fig. 2c and d, suggesting that ¹⁸O was exchanged between the H₂¹⁸O and CO₂ in the reaction chamber of the TGA before interacting with the sorbent. A comparison of the MS signals (in particular the ratio m/z 46/20) in Fig. 2e (mixing of CO₂ and H₂¹⁸O in the saturator) and Fig. 2f (mixing of CO₂ and H₂¹⁸O in the gas phase downstream of the saturator just before entering the reaction chamber of the TGA) hints that the mixing of CO₂ and H₂¹⁸O in the gas phase led to a slightly stronger oxygen exchange/ scrambling $(m/z \ 46/20 \approx 26$, compared to $m/z \ 46/20 \approx 20$ for

the mixing of CO_2 and $H_2^{18}O$ in the saturator). The ratio m/z 44/46 was ~10 and agreed reasonably well with the ratio of the nominal concentrations of CO_2 (15 vol%) and $H_2^{18}O$ (~1.6 vol%) in these experiments when most of the ¹⁸O has been exchanged between $H_2^{18}O$ and CO_2 . The initial peak of m/z 44 when switching from pure N_2 to 15 vol% CO_2/N_2 at the beginning of the CO_2 sorption stage was due to a short overshoot of the CO_2 flow rate when activating the mass flow controller (Fig. 2c-f). A corresponding spike in m/z 46 due to oxygen exchange (not due to the natural appearance of m/z 46 in CO_2 , as seen in Fig. 2c, d and Table 1) was observed only when CO_2 and $H_2^{18}O$ mixed in the saturator, because slightly more $H_2^{18}O$ was taken up by the larger flow of gas (Fig. 2e), but not when CO_2 and $H_2^{18}O$ mixed in the gas phase (Fig. 2f).

Interestingly, there was hardly any signal due to m/z 48 in any of the experiments shown in Fig. 2a–f, suggesting that the ¹⁸O in $\rm H_2$ ¹⁸O was exchanged with only one of the two ¹⁶O atoms in $\rm CO_2$; for $\rm C^{18}O_2$ to form through exchange reactions with $\rm H_2$ ¹⁸O, multiple collisions of the same $\rm CO_2$ molecule with $\rm H_2$ ¹⁸O would have been required that are unlikely given the plug flow-type gas flow pattern in the reaction chamber of the TGA (Fig. 1). This is reflected also in the Raman spectra of the carbonated samples in Fig. 3 (collected after 5 cycles plus an additional carbonation for 4 h to enhance the signal intensity due to $\rm CO_3$ ²⁻⁻ species, shown exemplarily in Fig. 3f). The samples carbonated under dry or humid ($\rm H_2$ ¹⁶O) conditions showed the most dominant

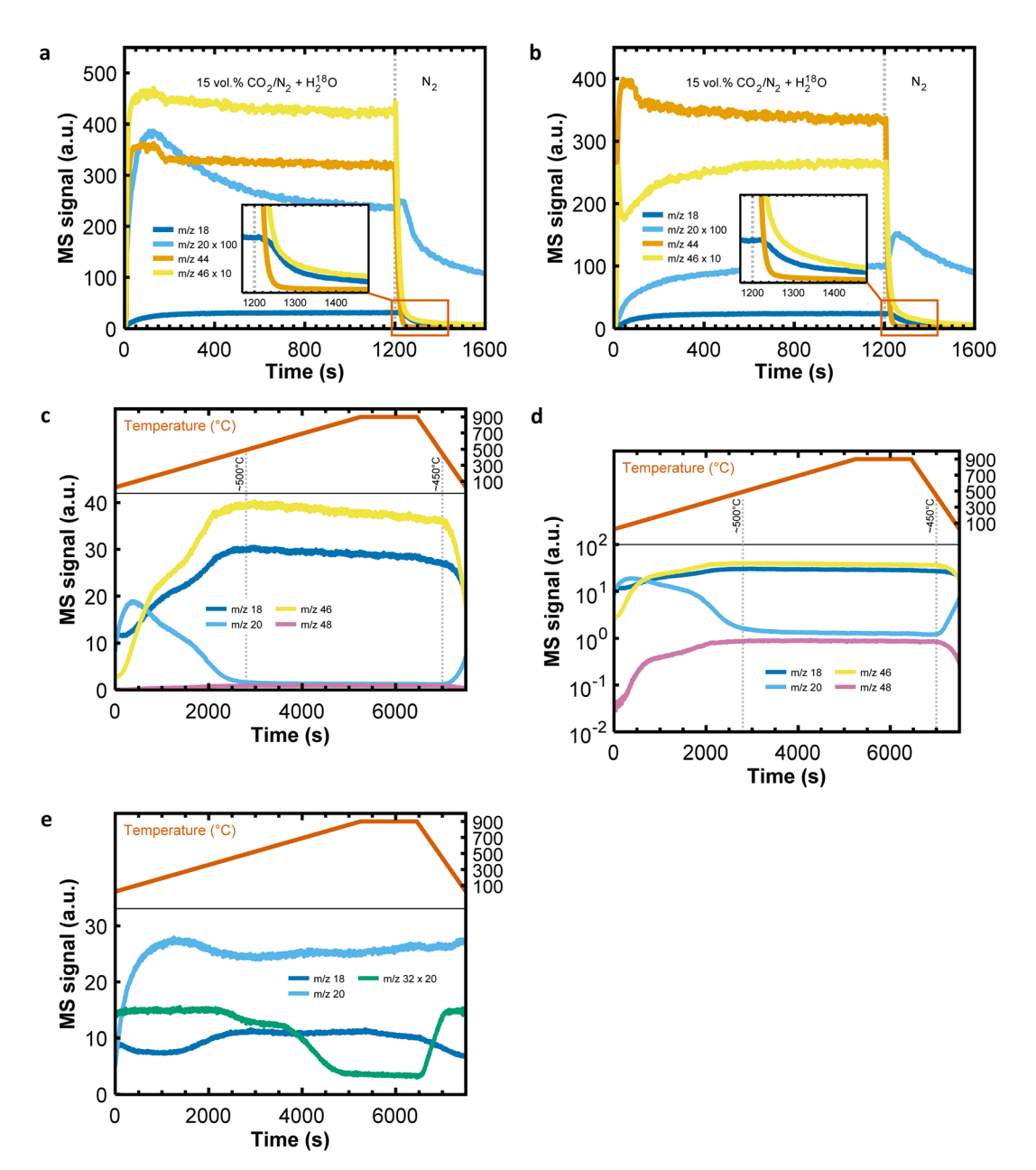


Fig. 5 Blank measurements (empty crucible) using the TGA-MS. (a) and (b) Show the MS signals corresponding to the experimental conditions in Fig. 2; in (a) both N_2 and CO_2 flowed through the saturator filled with labeled water ($H_2^{18}O$), whereas in (b) only N_2 flowed through the saturator. (c) and (d) MS signals showing the influence of temperature on the exchange of oxygen between H_2O and CO_2 when feeding a mixture of steam derived from labeled water ($H_2^{18}O$) and CO_2 ; in (c) the MS signals are plotted on a linear scale, whereas in (d) the MS signals are plotted on a logarithmic scale. (e) Influence of temperature on the stability of the MS signals due to water (M_2 18 and M_2 20) in the absence of CO_2 ; here, pure N_2 flowed through the saturator filled with a mixture of deionized water and labeled water ($H_2^{18}O$).

bands due to the ν_1 (\sim 1087 cm⁻¹), ν_4 (\sim 713 cm⁻¹), ν_{13} (\sim 281 cm⁻¹) and ν_{14} (\sim 153 cm⁻¹) vibrational modes of CO₃²⁻¹ species (Fig. 3a and b). The corresponding bands for the samples carbonated under humid conditions using $\rm H_2^{18}O$ were red shifted slightly, and an additional peak due to ^{18}O replacing one of the three ^{16}O atoms in the carbonate group was observed (ν_1 vibration, \sim 1063 cm⁻¹, Fig. 3c and d). Additional peaks near \sim 1050 cm⁻¹ and \sim 1030 cm⁻¹ would have been observed had more than one ^{18}O in the carbonate group been replaced; ⁴¹ the absence (or presence below the detection limit) of these peaks agrees well with the insignificance of the MS signal m/z 48 (see

control experiments in Fig. 5c and d). The XRD pattern in Fig. 3e confirms that the partially carbonated samples consisted of unconverted CaO and the calcite phase of CaCO₃ only, but not any other polymorph of CaCO₃ (*e.g.*, aragonite or vaterite), which might have produced similar additional ν_1 vibrations as the ¹⁸O in the carbonate group. ⁴⁰Considering that the sorbent was exposed to no more than ~1.5–2 vol% C¹⁶O¹⁸O (assuming an extreme case in which all ¹⁸O of H₂¹⁸O was exchanged with ¹⁶O in CO₂) and ~13–13.5 vol% C¹⁶O₂, it is interesting to note that the ratio of the peak areas due to CaCO₃ with zero ¹⁸O (CaC¹⁶O₃ at ~1087 cm⁻¹) to CaCO₃ with one ¹⁸O (CaC¹⁸O¹⁶O₂ at

 \sim 1063 cm⁻¹) was \sim four, *i.e.*, much lower than expected from the CO₂ isotope composition in the gas stream.

3.3 Implications for the goal of this study to understand the role of steam

The exchange of oxygen between H₂¹⁸O and CO₂ in the reaction chamber of the TGA is a problem for the examination of the promotional mechanism of steam for the carbonation reaction, because the presence of ¹⁸O in the CaCO₃ formed (or the release of ¹⁸O-containing CO₂ from the material upon decomposition) cannot be attributed solely to a reaction mechanism that involves steam (or its oxygen component); in fact, it is much more likely that the presence of ¹⁸O in CaCO₃ (as observed by Raman spectroscopy in Fig. 3c and d) originated from C¹⁶O¹⁸O rather than the remaining small quantity of H₂¹⁸O in the gas stream. Fig. 5c shows that the exchange of oxygen between ${\rm H_2}^{18}{\rm O}$ (here only ${\sim}0.1$ vol% due to the dilution of ${\rm H_2}^{18}{\rm O}$ with $H_2^{16}O$ (5:95) in the saturator) and CO_2 (15 vol%) is temperature-dependent, and with increasing temperature, more oxygen was exchanged between the two. 42 Above ~ 500 $^{\circ}$ C the ratios of the MS signals due to steam (m/z 18 and 20) and CO_2 (m/z 44, 46 and 48) remained constant. From Fig. 5e it is apparent that in the absence of ¹⁶O-containing gas species there

was no significant change in the intensity of the MS signal due to m/z 20. Traces of O₂ present in N₂ (\sim 80 ppm, m/z 32) appear to have exchanged 16 O with H₂ 18 O, but m/z 34 or m/z 36 were not measured in this experiment to confirm this observation.

Interestingly, the ratio m/z 18/20 \approx 22 above 500 °C (Fig. 5c) was an order of magnitude lower than ∼330 expected from Table 1 when assuming that ¹⁸O from H₂ ¹⁸O is exchanged to the level of its natural abundance in water; the short residence time (a few seconds) of the gas molecules in the high-temperature reaction chamber of the TGA may possibly have prevented an even higher degree of oxygen exchange to reach isotopic equilibrium. The lack of significant back-mixing in the reaction chamber of the TGA (as opposed to a closed system such as an autoclave), the fast rate of oxygen exchange above 500 °C, and the short gas residence time may have resulted in the exchange of only one ¹⁶O in the CO₂ molecule by H₂¹⁸O. The MS signal due to m/z 48 followed the same trend as m/z 46 (this is seen best when Fig. 5c is plotted on a logarithmic scale, Fig. 5d), indicating that indeed for a small fraction of CO2 molecules entering the reaction chamber of the TGA both ¹⁶O atoms in the CO₂ molecule were exchanged by two different H₂¹⁸O molecules; however, the high ratio m/z 46/48 \approx 42 shows that the exchange of only one oxygen atom in the CO2 molecule with H₂¹⁸O was dominant.

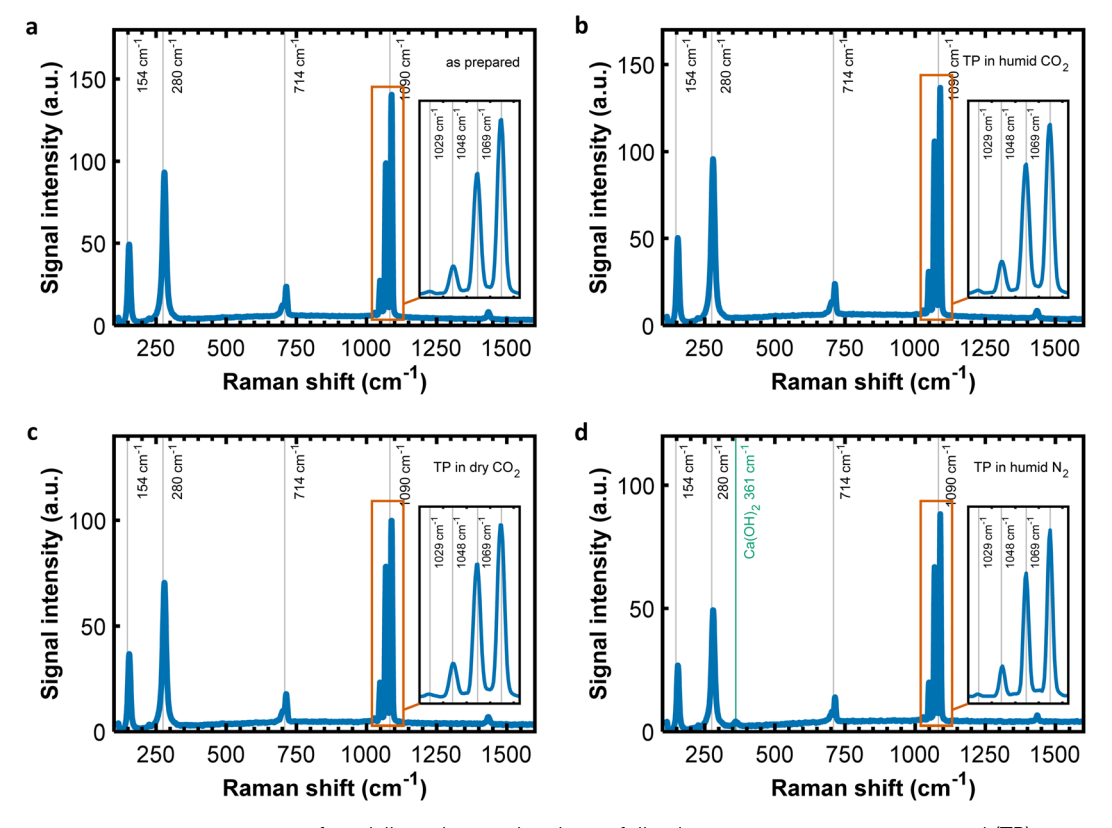


Fig. 6 Raman spectroscopy measurements of partially carbonated sorbents following a temperature-programmed (TP) treatment in a larger TGA under different conditions. (a) The partially carbonated sorbent was prepared by calcining $CaCO_3$ powder at 900 °C, followed by exposure to 5 vol% CO_2 and 2 vol% steam derived from labeled water ($H_2^{18}O$) at 700 °C for 12 h. The CO_2 uptake was 0.75 g CO_2 per g sorbent. (b) The material prepared in (a) was heated from room temperature to 600 °C in 5 vol% CO_2 and 2 vol% steam derived from deionized water. (c) The material prepared in (a) was heated from room temperature to 600 °C in 5 vol% CO_2 . (d) The material prepared in (a) was heated from room temperature to 600 °C in 2 vol% steam derived from deionized water. Ratio of peak areas ($CaC^{16}O_3$ at 1090 cm⁻¹ and $CaC^{18}O^{16}O_2$ at 1069 cm⁻¹): 1.4 (a), 1.3 (b), 1.3 (c) and 1.3 (d).

For completeness, we performed an additional series of experiments using a TGA with a larger reaction chamber (~46 ml) to facilitate back-mixing of the reaction gas, and thereby enhance the probability of oxygen exchange between H2O and CO₂ molecules. Commercial CaCO₃ powder (extra pure, Fisher Scientific) was calcined at 900 °C in N₂, followed by carbonation at 700 °C in steam (~2 vol%, derived from labeled water) and CO₂ (~5 vol%) for 12 h. Indeed, Raman spectroscopy revealed additional features of the v_1 vibration (Fig. 6a), indicating that the partially carbonated sorbent contained, in addition to the experiments performed in the smaller TGA, two and three ¹⁸O in the carbonate group.40 Upon further treatment of the material in atmospheres without ¹⁸O, there was no noticeable change in the ratio of peak areas in the v_1 region (CaC¹⁶O₃ at 1090 cm⁻¹ and CaC¹⁸O¹⁶O₂ at 1069 cm⁻¹), Fig. 6a-c. Thus, no measurable oxygen exchange occurred between gaseous CO2 and, or, H2O and the solid CaCO3 over the timescale and conditions of our experiments (for comparison see e.g., the work by Rosenbaum³⁴ who has reported carbon and oxygen isotope exchange for CO2 and CaCO₃ at 900 °C). The material treated in H₂O/N₂ decomposed slightly, explaining an additional Raman band due to $Ca(OH)_2$ in Fig. 6d. Interestingly, the small peak at 1029 cm⁻¹ in Fig. 6a-c originated from CaCO₃ containing three ¹⁸O (CaC¹⁸O₃). Since oxygen exchange between H₂¹⁸O and CO₂ in the high-temperature reaction chamber of the larger TGA yielded, at best, C18O2, a mixture of CaC18O216O, CaC18O16O2 and CaC¹⁶O₃ would be expected upon reaction with CaO. Thus, the results from Raman spectroscopy indicate that there must have been additional oxygen exchange between ¹⁸O-containing H₂O or CO₂ and the solid phases CaO or CaCO₃. With CO₃²⁻ diffusing through the CaCO3 product layer toward the CaO-CaCO₃ interface,²⁴ oxygen (and carbon) exchange would be expected as part of the volume/lattice diffusion mechanism (involving possibly recrystallization or Ostwald ripening),34,43,44 but this was not observed in our experiments (Fig. 6a-c) and therefore ruled out as an explanation for the formation of CaC¹⁸O₃. Given the relatively fast rates of carbonation under both dry and humid conditions (Fig. 2a and b), it is unlikely that volume/lattice diffusion was rate-controlling in our experiments.45 Instead, diffusion along grain boundaries or narrow pores (note that CaCO3 crystals formed during carbonation are far from perfect⁴⁶) may have dominated mass transport,⁴⁷ decreasing the likelihood of oxygen exchange between CO2/ CO₃²⁻ and CaCO₃.²⁶ It is thus possible that the presence of three ¹⁸O in CaCO₃ originates from oxygen exchange with CaO. CO₂ would immediately form CaCO3 when in contact with CaO, implying that H2O is responsible for the exchange of oxygen with CaO that results in the formation of CaC¹⁸O₃ upon further reaction with C18O2. Similar results have been reported previously, suggesting that steam can interact with CaO above the decomposition temperature of Ca(OH)2.38 Whether the oxygen exchange between steam and CaO under reaction conditions contributes to the accelerated rates of CO₂ uptake remains, however, uncertain but may motivate future research activities. The presence of steam alters the dominant transport mechanism of species required to form CaCO3 (viz. carbon and

due to the challenging reaction conditions and the relatively short timescale of the carbonation reaction. From the absence of measurable oxygen exchange between H₂O or CO₂ and CaCO₃ we conclude that volume/lattice diffusion appears to play a negligible role in the carbonation reaction using limestone-derived particles, and therefore many mechanisms discussed in the literature such as the hydrolyzation and weakening of C-O bonds in CaCO₃ through protons, or the faster OH⁻ diffusion over O²⁻ diffusion through CaCO₃ may not apply under relevant reaction conditions.

Investigations of oxygen isotope exchange may not be suited to unveil the enhancement effect of steam during the carbonation of CaO at high temperatures, as there will always be oxygen exchange between the gaseous oxygen-containing reactants. The intrinsic properties of steam causing the acceleration of CO₂ uptake cannot be linked with the oxygen or hydrogen components, and oxygen atoms originating from the water molecule will inevitably end up in the CaCO₃ product through different sequences of oxygen exchange. However, our experiments did provide insights into the presence or absence of oxygen exchange between the gas and solid components involved in the carbonation reaction, from which information on the relevant transport processes can be obtained.

4. Conclusions

In calcium looping, the presence of steam is known to accelerate the rate of CO₂ uptake. We designed experiments in which steam derived from labeled water (H₂¹⁸O) was used to promote CO2 sorption in a TGA, and tracked 18O in gaseous and solid products through mass spectrometry and Raman spectroscopy to obtain mechanistic insights into the enhancement effect, for example whether oxygen contained in steam contributes directly to carbonate formation. While we indeed observed the incorporation of ¹⁸O into the calcite structure (and the release of ¹⁸O-containing CO₂ in the subsequent decomposition step), we found that most of 18O contained in labelled water was exchanged with ¹⁶O contained in CO₂ in the high-temperature reaction chamber of the TGA before reaching the sorbent. Thus, the CO₂ contained a substantial fraction of ¹⁸O before reacting with CaO to form CaCO₃ that contained ¹⁸O. The degree of oxygen exchange between H2O and CO2 depended greatly on temperature, but also the contact time and the gas flow pattern in the high-temperature reaction chamber of the TGA. With the given reaction conditions and our experimental setup, it was not possible to eliminate oxygen exchange between H₂O and CO₂ completely. Using a larger TGA furnace facilitated back-mixing of gas and increased its residence time in the TGA, which in turn enhanced the degree of oxygen exchange such that not only $C^{18}O^{16}O$ but also $C^{18}O_2$ was formed. Consequently, Raman spectroscopy revealed the formation of CaCO₃ with zero, one, two and three ¹⁸O atoms in the carbonate group.

Although the use of labelled water/steam was not suitable under the given reaction conditions to obtain unequivocal insight into why steam accelerates CO₂ uptake, oxygen interactions between solid and gas phases could be probed. Our results indicate that there is no oxygen exchange between solid

oxygen),48 but its identification and quantification is difficult

 $CaCO_3$ and H_2O/CO_2 under reaction conditions relevant to calcium looping. However, oxygen exchange appears to occur between solid CaO and H_2O , which may contribute to the enhancement effect of steam, and motivate further investigations.

Conflicts of interest

There are no conflicts to declare.

Data availability

All data presented in Fig. 2–6 is available through the Zenodo repository (10.5281/zenodo.17395250).

References

- 1 J. Chen, L. Duan and Z. Sun, Review on the Development of Sorbents for Calcium Looping, *Energy Fuels*, 2020, **16**, 7806–7836, DOI: 10.1021/acs.energyfuels.0c00682.
- 2 C. Wu, Q. Huang, Z. Xu, A. T. Sipra, N. Gao, L. P. d. S. Vandenberghe, S. Vieira, C. R. Soccol, R. Zhao and S. Deng, *et al.*, A Comprehensive Review of Carbon Capture Science and Technologies, *Carbon Capture Science and Technology*, Elsevier Ltd, 2024, DOI: 10.1016/j.ccst.2023.100178.
- 3 M. T. Dunstan, F. Donat, A. H. Bork, C. P. Grey and C. R. Müller, CO2 Capture at Medium to High Temperature Using Solid Oxide-Based Sorbents: Fundamental Aspects, Mechanistic Insights, and Recent Advances, *Chem. Rev.*, 2021, 27, 12681–12745, DOI: 10.1021/acs.chemrev.1c00100.
- 4 J. Moreno, M. Hornberger, M. Schmid and G. Scheffknecht, Part-Load Operation of a Novel Calcium Looping System for Flexible CO2 Capture in Coal-Fired Power Plants, *Ind. Eng. Chem. Res.*, 2021, **60**(19), 7320–7330, DOI: **10.1021**/acs.iecr.1c00155.
- 5 J. Ströhle, J. Hilz and B. Epple, Performance of the Carbonator and Calciner during Long-Term Carbonate Looping Tests in a 1 MWth Pilot Plant, *J. Environ. Chem. Eng.*, 2020, **8**(1), DOI: **10.1016/j.jece.2019.103578**.
- 6 B. Arias, Y. Alvarez Criado, A. Méndez, P. Marqués, I. Finca and J. C. Abanades, Pilot Testing of Calcium Looping at TRL7 with CO2 Capture Efficiencies toward 99%, *Energy Fuels*, 2024, 38(15), 14757–14764, DOI: 10.1021/ acs.energyfuels.4c02472.
- 7 A. Otto, T. Grube, S. Schiebahn and D. Stolten, Closing the Loop: Captured CO2 as a Feedstock in the Chemical Industry, *Energy Environ. Sci.*, 2015, **8**(11), 3283–3297, DOI: **10.1039/c5ee02591e**.
- 8 W. Gao, S. Liang, R. Wang, Q. Jiang, Y. Zhang, Q. Zheng, B. Xie, C. Y. Toe, X. Zhu, J. Wang, *et al.*, Industrial Carbon Dioxide Capture and Utilization: State of the Art and Future Challenges, *Chem. Soc. Rev.*, 2020, 7, 8584–8686, DOI: 10.1039/d0cs00025f.
- 9 F. Donat, N. H. Florin, E. J. Anthony and P. S. Fennell, Influence of High-Temperature Steam on the Reactivity of CaO Sorbent for CO2 Capture, *Environ. Sci. Technol.*, 2012, 46(2), 1262–1269, DOI: 10.1021/es202679w.

- 10 S. Zhang, S. He, N. Gao, C. Quan and C. Wu, Effect of Steam Addition for Energy Saving during CaCO3 Calcination of Auto Thermal Biomass Gasification, *Biomass Bioenergy*, 2022, 161, DOI: 10.1016/j.biombioe.2022.106416.
- 11 J. Arcenegui-Troya, P. E. Sánchez-Jiménez, A. Perejón, V. Moreno, J. M. Valverde and L. A. Pérez-Maqueda, Kinetics and Cyclability of Limestone (CaCO3) in Presence of Steam during Calcination in the CaL Scheme for Thermochemical Energy Storage, *Chem. Eng. J.*, 2021, 417, DOI: 10.1016/j.cej.2021.129194.
- 12 G. Giammaria and L. Lefferts, Catalytic Effect of Water on Calcium Carbonate Decomposition, *J. CO*₂ *Util.*, 2019, 33, 341–356, DOI: 10.1016/j.jcou.2019.06.017.
- 13 M. Silakhori, M. Jafarian, A. Chinnici, W. Saw, M. Venkataraman, W. Lipiński and G. J. Nathan, Effects of Steam on the Kinetics of Calcium Carbonate Calcination, *Chem. Eng. Sci.*, 2021, 246, DOI: 10.1016/j.ces.2021.116987.
- 14 J. Arcenegui-Troya, P. E. Sánchez-Jiménez, A. Perejón, J. M. Valverde and L. A. Pérez-Maqueda, Steam-Enhanced Calcium-Looping Performance of Limestone for Thermochemical Energy Storage: The Role of Particle Size, J. Energy Storage, 2022, 51, DOI: 10.1016/j.est.2022.104305.
- 15 J. Dong, Y. Tang, A. Nzihou and E. Weiss-Hortala, Effect of Steam Addition during Carbonation, Calcination or Hydration on Re-Activation of CaO Sorbent for CO2 Capture, J. CO₂ Util., 2020, 39, DOI: 10.1016/ j.jcou.2020.101167.
- 16 N. Rong, J. Wang, K. Liu, L. Han, Z. Mu, X. Liao and W. Meng, Enhanced CO2 Capture Durability and Mechanical Properties Using Cellulose-Templated CaO-Based Pellets with Steam Injection during Calcination, *Ind. Eng. Chem. Res.*, 2023, 62(3), 1533–1541, DOI: 10.1021/ acs.iecr.2c03746.
- 17 N. Rong, J. Wang, L. Han, Y. Wu, Z. Mu, X. Wan and G. Wang, Effect of Steam Addition during Calcination on CO2 Capture Performance and Strength of Bio-Templated Ca-Based Pellets, *J. CO₂ Util.*, 2022, 63, DOI: 10.1016/ j.jcou.2022.102127.
- 18 S. Champagne, D. Y. Lu, A. MacChi, R. T. Symonds and E. J. Anthony, Influence of Steam Injection during Calcination on the Reactivity of CaO-Based Sorbent for Carbon Capture, *Ind. Eng. Chem. Res.*, 2013, 52(6), 2241– 2246, DOI: 10.1021/ie3012787.
- 19 L. Zhang, B. Zhang, Z. Yang and M. Guo, The Role of Water on the Performance of Calcium Oxide-Based Sorbents for Carbon Dioxide Capture: A Review, *Energy Technol.*, 2015, 3(1), 10–19, DOI: 10.1002/ente.201402099.
- 20 J. Zha, Y. Yan, P. Ma, Y. Huang, F. Qi, X. Liu, R. Diao and D. Yan, The Role of Water Vapour on CO2 Mobility on Calcite Surface during Carbonation Process for Calcium Looping: A DFT Study, *Carbon Capture Sci. Technol.*, 2024, 12, DOI: 10.1016/j.ccst.2024.100226.
- 21 Y. Fan, J. G. Yao, Z. Zhang, M. Sceats, Y. Zhuo, L. Li, G. C. Maitland and P. S. Fennell, Pressurized Calcium Looping in the Presence of Steam in a Spout-Fluidized-Bed Reactor with DFT Analysis, *Fuel Process. Technol.*, 2018, 169, 24–41, DOI: 10.1016/j.fuproc.2017.09.006.

- 22 H. Wang, Z. Li and N. Cai, Multiscale Model for Steam Enhancement Effect on the Carbonation of CaO Particle, *Chem. Eng. J.*, 2020, **394**, DOI: **10.1016/j.cej.2020.124892**.
- 23 Z. Li, Y. Liu and N. Cai, Understanding the Enhancement Effect of High-Temperature Steam on the Carbonation Reaction of CaO with CO2, *Fuel*, 2014, **127**, 88–93, DOI: **10.1016/j.fuel.2013.06.040**.
- 24 Z. Sun, S. Luo, P. Qi and L. S. Fan, Ionic Diffusion through Calcite (CaCO3) Layer during the Reaction of CaO and CO2, *Chem. Eng. Sci.*, 2012, 81, 164–168, DOI: 10.1016/ j.ces.2012.05.042.
- 25 J. Ruan, C. Gao, T. Deng and C. Qin, Understanding the Influences and Mechanism of Water Vapor on CO2 Capture by High-Temperature Li4SiO4 Sorbents, *Sep. Purif. Technol.*, 2025, 354, DOI: 10.1016/j.seppur.2024.129289.
- 26 J. R. Farver and R. A. Yund, Measurement of Oxygen Grain Boundary Diffusion in Natural, Fine-Grained, Quartz Aggregates, *Geochim. Cosmochim. Acta*, 1991, 55, 1597– 1607, DOI: 10.1016/0016-7037(91)90131-N.
- 27 J. R. Farver, Oxygen and Hydrogen Diffusion in Minerals, *Rev. Mineral. Geochem.*, 2010, 72, 447–507, DOI: 10.2138/rmg.2010.72.10.
- 28 A. K. Kronenberg, R. A. Yund and B. J. Giletti, Carbon and Oxygen Diffusion in Calcite: Effects of Mn Content and PH2O, *Phys. Chem. Miner.*, 1984, **11**, 101–112, DOI: **10.1007/BF00309248**.
- 29 J. R. Farver and R. A. Yund, Oxygen Diffusion in Quartz: Dependence on Temperature and Water Fugacity, *Chem. Geol.*, 1991, 90, 55–70, DOI: 10.1016/0009-2541(91)90033-N.
- 30 J. R. Farver, Oxygen Self-Diffusion in Calcite: Dependence on Temperature and Water Fugacity, *Earth Planet. Sci. Lett.*, 1994, 121, 575–587, DOI: 10.1016/0012-821X(94)90092-2.
- 31 Y. Zhang, E. M. Stolper and G. J. Wasserburg, Diffusion of a Multi-Species Component and Its Role in Oxygen and Water Transport in Silicates, *Earth Planet. Sci. Lett.*, 1991, 103, 228–240, DOI: 10.1016/0012-821X(91)90163-C.
- 32 T. C. Labotka, D. R. Cole, M. J. Fayek and T. Chacko, An Experimental Study of the Diffusion of C and O in Calcite in Mixed CO2-H2O Fluid, *Am. Mineral.*, 2011, **96**(8–9), 1262–1269, DOI: **10.2138/am.2011.3738**.
- 33 D. C. Brenner, B. H. Passey and D. A. Stolper, Influence of Water on Clumped-Isotope Bond Reordering Kinetics in Calcite, *Geochim. Cosmochim. Acta*, 2018, **224**, 42–63, DOI: **10.1016/j.gca.2017.12.026**.
- 34 J. M. Rosenbaum, Stable Isotope Fractionation between Carbon Dioxide and Calcite at 900°C, *Geochim. Cosmochim. Acta*, 1994, **58**(17), 3747–3753, DOI: **10.1016/0016-7037(94) 90164-3**.
- 35 F. Donat and C. R. Müller, A Critical Assessment of the Testing Conditions of CaO-Based CO2 Sorbents, *Chem. Eng. J.*, 2018, 336, 544–549, DOI: 10.1016/j.cej.2017.12.050.
- 36 NIST Mass Spectrometry Data Center. Mass Spectra, in *NIST Chemistry WebBook*, NIST Standard Reference Database Number 69, ed. Linstrom, P. J. and Mallard, W. G.,

- National Institute of Standards and Technology, Gaithersburg MD, 2024.
- 37 G. S. Grasa and J. C. Abanades, CO2 Capture Capacity of CaO in Long Series of Carbonation/Calcination Cycles, *Ind. Eng. Chem. Res.*, 2006, 45(26), 8846–8851, DOI: 10.1021/ie0606946.
- 38 L. Thum, M. Rudolph, R. Schomäcker, Y. Wang, A. Tarasov, A. Trunschke and R. Schlögl, Oxygen Activation in Oxidative Coupling of Methane on Calcium Oxide, *J. Phys. Chem. C*, 2019, 123(13), 8018–8026, DOI: 10.1021/acs.jpcc.8b07391.
- 39 A. Landuyt, P. V. Kumar, J. A. Yuwono, A. H. Bork, F. Donat, P. M. Abdala and C. R. Müller, Uncovering the CO2 Capture Mechanism of NaNO3-Promoted MgO by 18O Isotope Labeling, *JACS Au*, 2022, 2(12), 2731–2741, DOI: 10.1021/jacsau.2c00461.
- 40 M. De La Pierre, C. Carteret, L. Maschio, E. André, R. Orlando and R. Dovesi, The Raman Spectrum of CaCO3 Polymorphs Calcite and Aragonite: A Combined Experimental and Computational Study, *J. Chem. Phys.*, 2014, 140(16), DOI: 10.1063/1.4871900.
- 41 P. Gillet, P. McMillan, J. Schott, J. Badro and A. Grzechnik, Thermodynamic Properties and Isotopic Fractionation of Calcite from Vibrational Spectroscopy of 18O-Substituted Calcite, *Geochim. Cosmochim. Acta*, 1996, **60**(18), 3471–3485, DOI: **10.1016/0016-7037(96)00178-0**.
- 42 G. Chiodini, P. Allard, S. Caliro and F. Parello, 18O Exchange between Steam and Carbon Dioxide in Volcanic and Hydrothermal Gases: Implications for the Source of Water, *Geochim. Cosmochim. Acta*, 2000, **64**(14), 2479–2488, DOI: **10.1016/S0016-7037(99)00445-7**.
- 43 D. R. Cole and S. Chakraborty, Rates and Mechanisms of Isotopic Exchange, *Rev. Mineral. Geochem.*, 2001, 43(1), 83–223, DOI: 10.2138/gsrmg.43.1.83.
- 44 T. Chacko, T. K. Mayeda, R. N. Clayton and J. R. Goldsmith, Oxygen and Carbon Isotope Fractionations between CO2 and Calcite, *Geochim. Cosmochim. Acta*, 1991, **55**, 2867–2882, DOI: **10.1016/0016-7037(91)90452-B**.
- 45 M. Krödel, D. Spescha, A. Kierzkowska, F. Donat and C. R. Müller, Experimental and Numerical Investigation of the Morphological Changes of a Natural Limestone-Based CO2 Sorbent over Repeated Carbonation-Calcination Cycles, Carbon Capture Sci. Technol., 2025, 16, 100486, DOI: 10.1016/j.ccst.2025.100486.
- 46 D. Mess, A. F. Sarofim and J. P. Longwell, Product Layer Diffusion during the Reaction of Calcium Oxide with Carbon Dioxide, *Energy Fuels*, 1999, 13(5), 999–1005, DOI: 10.1021/ef980266f.
- 47 J. R. Farver and R. A. Yund, Oxygen Grain Boundary Diffusion in Natural and Hot-Pressed Calcite Aggregates, *Earth Planet. Sci. Lett.*, 1998, 161, 189–200, DOI: 10.1016/ S0012-821X(98)00150-2.
- 48 J. R. Farver and R. A. Yund, Oxygen Diffusion in a Fine-Grained Quartz Aggregate with Wetted and Nonwetted Microstructures, *J. Geophys. Res.*, 1992, 97(B10), 14017–14029, DOI: 10.1029/92jb01206.